J. Anat. (1980), **131**, 4, pp. 621–633
With 5 figures
Printed in Great Britain

An ultrastructural investigation of afferent connections of the red nucleus in the rat

B. A. FLUMERFELT

Department of Anatomy, The University of Western Ontario, London, Canada

(*Accepted* 17 *April* 1980)

INTRODUCTION

Although the synaptic organization of the red nucleus in the rat has been described (Reid, Flumerfelt & Gwyn, 1975) and its afferent pathways have been studied by light microscopic methods (Gwyn & Flumerfelt, 1974; Brown, 1974; Caughell & Flumerfelt, 1977; Flumerfelt & Caughell, 1978), little information is available concerning the ultrastructural features of its afferent connections. In the cat and monkey it is generally agreed that afferents from the sensorimotor cortex terminate throughout most of the red nucleus, including the magnocellular region which gives rise to the rubrospinal tract (Rinvik & Walberg, 1963; Mabuchi & Kusama, 1966; Kuypers & Lawrence, 1967). In the rat, however, the corticorubral projection terminates entirely within the parvocellular part of the nucleus which does not project down the spinal cord (Gwyn & Flumerfelt, 1974; Brown, 1974). The magnocellular part of the rat red nucleus receives its afferents almost entirely from the nucleus interpositus anterior of the cerebellum whose terminal field does not overlap with either cortical or dentate inputs to the red nucleus (Caughell & Flumerfelt, 1977). The functional organization of the red nucleus in the rat therefore differs from that in other species in certain fundamental respects and this difference is probably reflected in differences at the ultrastructural level. It was therefore undertaken to examine the ultrastructural pattern of degeneration within the red nucleus of the rat following cerebellar and cerebrocortical lesions, and to correlate the synaptic organization with the functional organization of the nucleus as a whole.

MATERIALS AND METHODS

Adult male Wistar rats weighing from 200 to 250 g were used in this study. All operations and perfusions were performed under sodium pentobarbital (Nembutal) anaesthesia. Anaesthetized animals were placed in a stereotaxic frame and the sensorimotor cortex or cerebellum was exposed. Using electrocautery, lesions were placed in various areas of the cerebral cortex to involve both the motor and sensory areas, the motor area alone, or the somatosensory area alone. In other animals electrolytic lesions were placed in the cerebellar nuclei or brachium conjunctivum by stereotaxic methods (Caughell & Flumerfelt, 1977). Following closure of the wound, most of the animals were allowed to survive for 1–7 days. In addition, a few animals were kept for longer survival periods up to 3 months in duration. When killed, all animals were anaesthetized and then injected with a mixture of 1 % sodium nitrite (10 mg/kg) and heparin (50 units/kg) at least 5 minutes prior to perfusion to achieve vasodilatory and anticoagulant effects respectively. Prior to use all perfusion fluid

0021-8782/80/2828-8340 $02.00

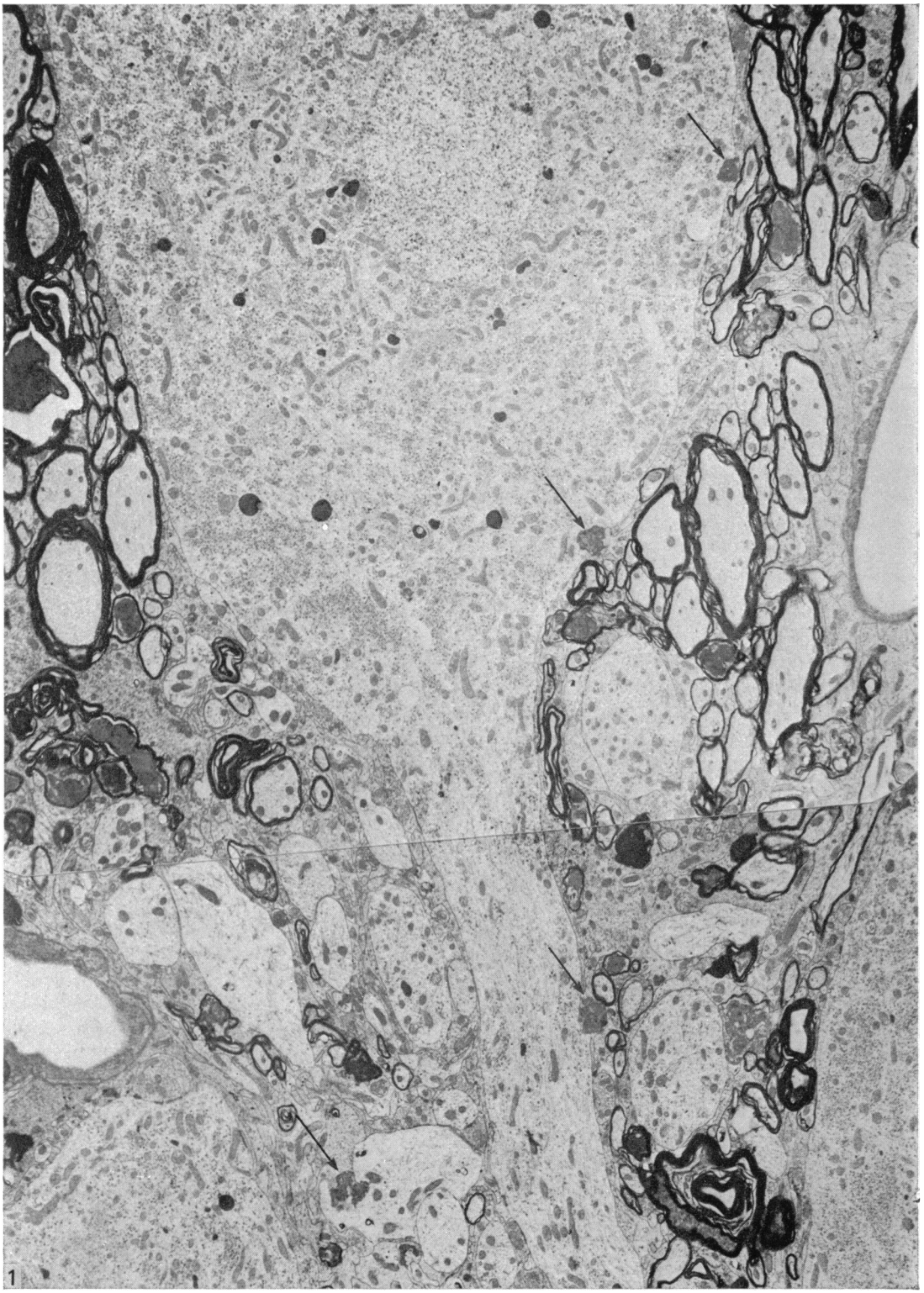

Fig. 1. Electron micrograph montage showing several dark degenerating terminal profiles (arrows) in association with the cell body of a magnocellular neuron and two proximal dendrites. Note the presence of numerous degenerating myelinated fibres containing electron-dense axoplasm. 3 days. × 4500.

was warmed to 37 °C and a 5 % CO_2/95 % O_2 mixture was bubbled through it for 15 minutes. The animals were then perfused intracardially with a solution of 0·5 % pure glutaraldehyde and 4 % paraformaldehyde (Vaughn & Peters, 1966) in cacodylate buffer. After perfusion the brain was left *in situ* overnight at 4 °C and then removed.

The extent of the cortical lesions was observed and plotted with reference to the maps of the cortical areas provided by Kreig (1946), Woolsey (1952, 1958), Barnard & Woolsey (1956) and Welker (1971). Lesions in the cerebellar nuclei or brachium conjunctivum were evaluated in Nissl-stained frozen sections through the cerebellum.

In all cases with suitable lesions, the midbrains were sliced into 100–200 μm sections in the transverse plane using a device described by Lewis & Shute (1966). The sections were next washed in 0·2 M cacodylate buffer at pH 7·4 and then immersed in a 1 % solution of osmium tetroxide in 0·2 M cacodylate buffer until the contours of the red nucleus became apparent. The nucleus in each section was dissected out, osmicated for 3 hours and then stained *en bloc* in a saturated aqueous solution of uranyl acetate for 4–5 hours. The tissue was dehydrated in a graded series of methyl alcohols, cleared in propylene oxide and flat embedded in 'Epon 812' (Luft, 1961), 'Spurr' (Spurr, 1969), or Epon–Araldite. To assist in identifying the portion of the nucleus contained in each block, semithin (1 μm) plastic sections were cut from the block face and stained with Mallory's azure II–methylene blue (Richardson, Jarett & Finke, 1960). Thin sections were then cut and stained with lead citrate (Reynolds, 1963) and examined with an A.E.I. EM 6B electron microscope.

OBSERVATIONS

The red nucleus in the rat is well separated into a caudal magnocellular region and a rostral parvocellular portion. Giant (> 40 μm diameter) and large (26–40 μm diameter) neurons were located predominantly within the magnocellular region of the red nucleus, and medium sized (20–25 μm diameter) and small (> 20 μm diameter) neurons predominated within the parvocellular part. In the magnocellular portion of the nucleus, the axons of the brachium conjunctivum were aggregated into large bundles which coursed between the cells. In regions where these fibre bundles were not as prominent, dendritic profiles of variable size and irregular contour occupied the neuropil. In the parvocellular portion the coursing fibre bundles of the brachium conjunctivum were not as evident and the dendritic profiles were not as large as those observed in the neuropil of the magnocellular region.

Three main types of synaptic terminals occurred in the red nucleus: (1) small terminals with flattened vesicles and symmetrical densities (F terminals), (2) small terminals with rounded vesicles and asymmetrical densities (RS terminals) and (3) large terminals with rounded vesicles and asymmetrical densities (RL terminals). RL terminals were restricted to the somata and proximal dendrites of giant and large magnocellular neurons. RS terminals and F terminals were found throughout the entire red nucleus and were located on somata, proximal and distal dendrites.

Cerebellar lesions

Material examined 3 days following cerebellar lesions revealed the greatest abundance of degenerating myelinated axons and electron-dense terminal profiles. The degenerating fibres of the brachium conjunctivum were of irregular contour and contained electron-dense axoplasm which was observed to be separated from the

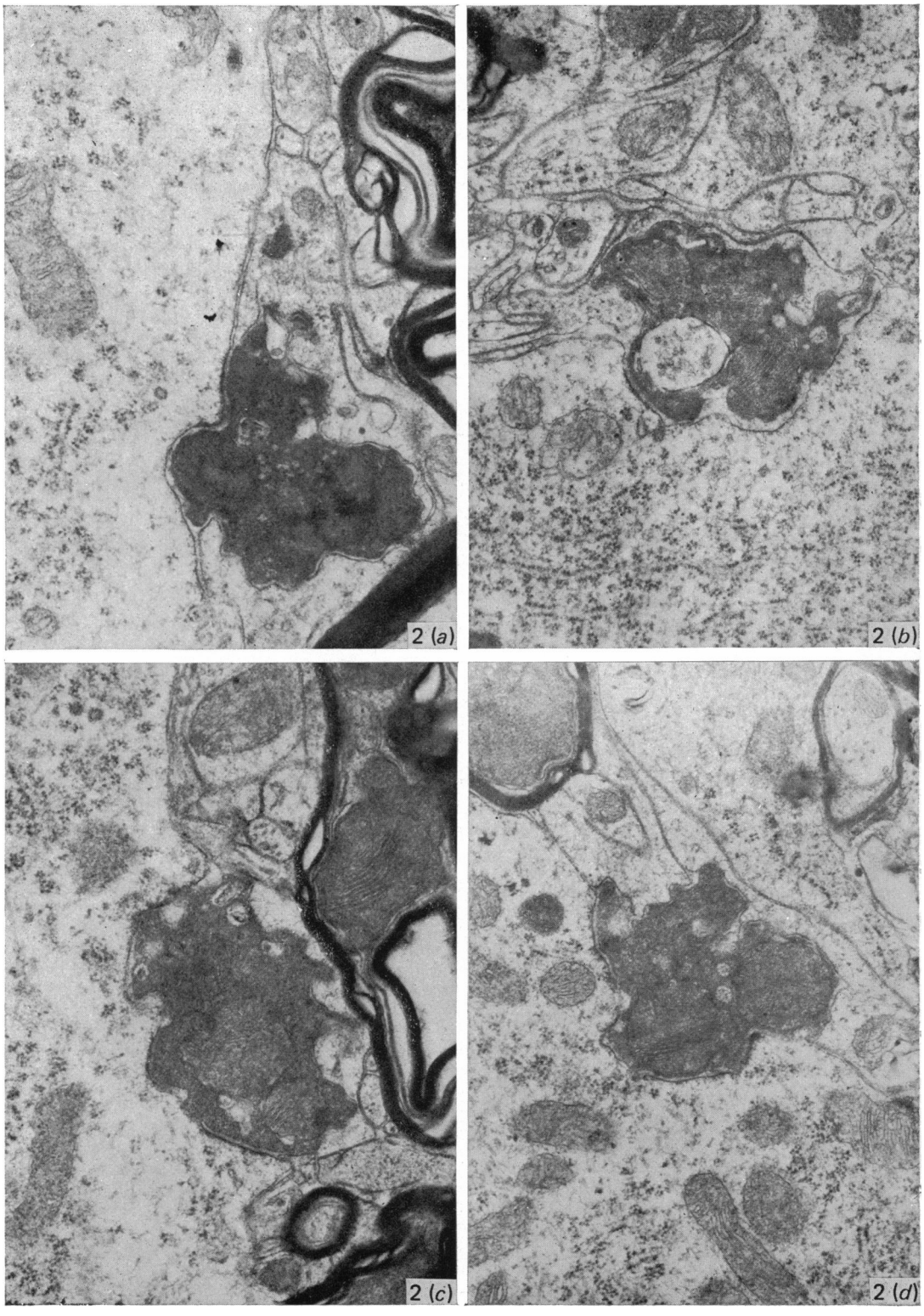
2 (a)
2 (b)
2 (c)
2 (d)

encompassing myelin (Figs. 1, 3*a*). Following destruction of both the nucleus lateralis and the nucleus interpositus, electron-dense terminal and pre-terminal degeneration was located throughout the entire contralateral red nucleus, with a greater abundance in the magnocellular portion than in the parvocellular region. Degenerating fibres were also more numerous in the medial half of the nucleus and became less apparent as the lateral regions were examined. Degenerating axons of cerebellar origin were largely myelinated, possessed darkened, granulated axoplasm and did not contain a normal content of neurofilaments, microtubules or mitochondria.

Magnocellular red nucleus

Degenerating terminal boutons of the magnocellular region possessed an electron-dense matrix and asymmetrical densities. The terminals were irregular in contour and were observed to be in contact with the somata (Fig. 2*a*, *b*) and proximal dendrites (Fig. 2*c*, *d*) of magnocellular neurons located throughout the caudal third of the red nucleus (Fig. 1). Degenerating terminal profiles possessed a finely granulated matrix with altered mitochondria and rounded synaptic vesicles. The mitochondria of degenerating terminals, when visible, appeared enlarged and possessed an electron-dense matrix with thin, elongated cristae (Fig. 2*a*, *c*). At more advanced stages of degeneration, both mitochondria and synaptic vesicles possessed disrupted membranes. Occasionally, vacuoles with diameters of 80–100 nm were seen within the degenerating boutons (Fig. 2*b*). Several of the degenerating profiles were partially or totally surrounded by glial processes.

Although degenerating terminal boutons located within the magnocellular region were found predominantly on cell bodies and proximal dendrites, they were occasionally found to be associated with medium sized dendrites. Terminals of this type were observed to occur in clusters of four to six and each was seen to be in contact with a separate dendritic profile (Fig. 3*a*).

Parvocellular red nucleus

Following a total unilateral lesion, the contralateral parvocellular region of the red nucleus contained both degenerating myelinated axons and electron-dense terminals. Degenerating fibre bundles within the parvocellular region were not as coarse as those observed in the medial aspect of the magnocellular region and degenerating terminals, although not as numerous, were similar to those viewed in the magnocellular portion. Both degenerating axons and terminal profiles were characterized by an electron-dense matrix with enlarged or lysed mitochondria and ruptured vesicles. These cerebellorubral endings which underwent an electron-dense

---

Fig. 2 (*a*) Electron micrograph showing a degenerating axosomatic terminal of irregular contour, possessing an electron-dense matrix and surrounded by glial cytoplasm. This degenerating profile contains enlarged mitochondria and a prominent post-synaptic density is evident. 3 days. × 31000. (*b*) Electron micrograph of a degenerating axosomatic terminal containing altered mitochondria and a large electron-translucent membrane-bound vacuole which possesses pleomorphic vesicles. This dark terminal is characterized by an asymmetrical synaptic density and is surrounded by glial cytoplasm. 3 days. × 28000. (*c*) Electron micrograph showing two degenerating fibres of passage and a degenerating axodendritic profile. This characteristic cerebellorubral terminal is undergoing electron-dense degeneration and possesses electron-opaque vacuoles and enlarged mitochondria which fill much of the degenerating bouton. 3 days. × 31000. (*d*) Electron micrograph of an axodendritic profile which resides in a depression of the plasma membrane and is undergoing electron-dense degeneration. Note the enlarged mitochondria and the glial processes surrounding the degenerating profile. 3 days. × 28000.

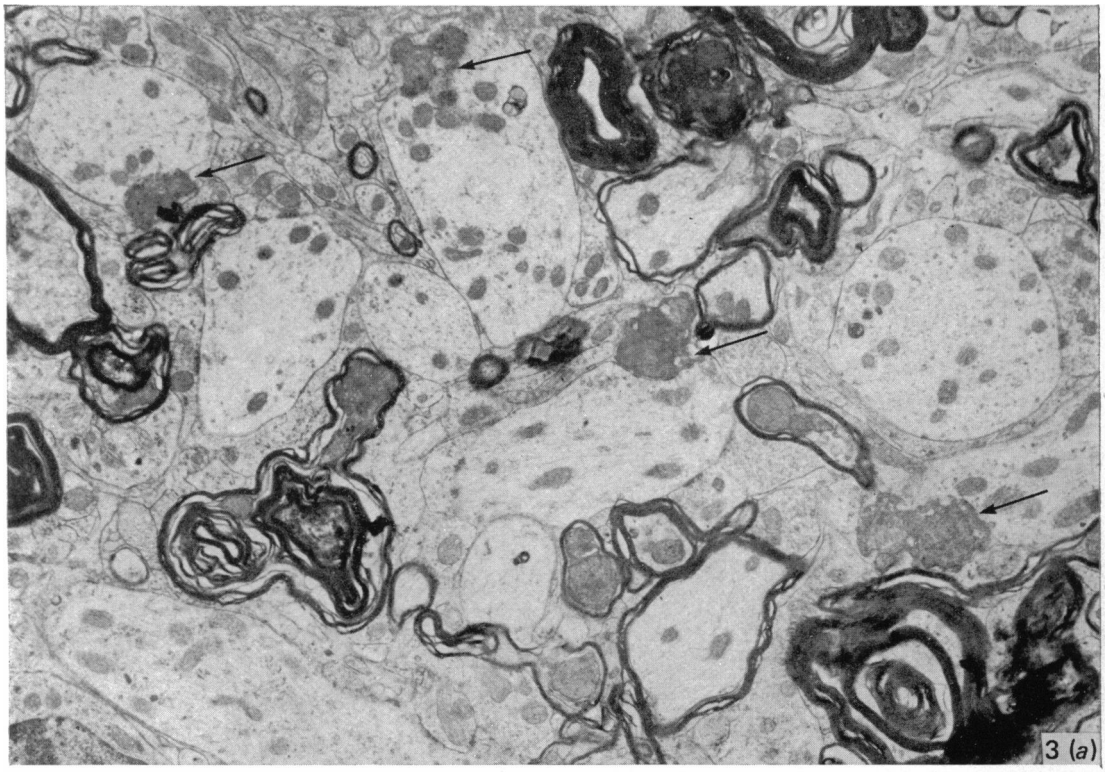

3 (*a*)

3 (*b*)

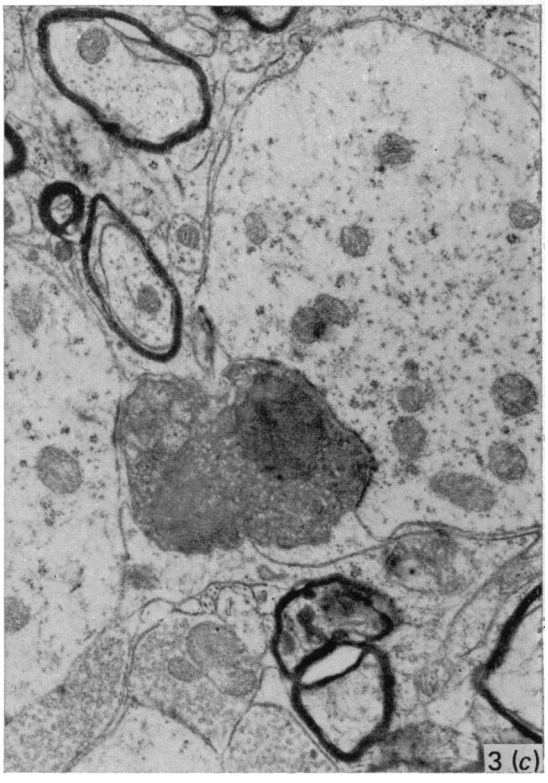

3 (*c*)

type of degeneration were seen primarily in contact with small to medium sized dendrites (Fig. 3*b*, *c*). Occasionally, a dark synaptic profile was seen in contact with the soma of a medium sized, parvocellular neuron. The synaptic densities of these endings were asymmetrical in type. Occasionally, it could be seen that the synaptic vesicles in these terminals were primarily spherical in shape, with some of them appearing amorphous and swollen.

Long term

Another type of terminal, characteristic of the magnocellular red nucleus, is very large, contains round vesicles and measures up to 15 μm in greatest dimension (Reid, Flumerfelt & Gwyn, 1975). Electron microscopic observations revealed that although the location of these RL terminals was similar to the interpositorubral endings, they were never found to be affected by lesions involving the deep cerebellar nuclei and the brachium conjunctivum at any time up to 3 months post-operatively (Fig. 4).

Cerebrocortical lesions

Electron microscopic examination of the red nucleus following lesions of the sensorimotor cortex revealed a sparse distribution of degenerating fibres in the parvocellular part of the nucleus. In some of these fibres disruption of the myelin sheath occurred. Small degenerating terminals undergoing an electron-dense type of degeneration were seen terminating on distal dendrites and spines (Fig. 5*a–d*). As early as 3 days post-operatively dense changes were visible, although it was still possible to identify the shape of the synaptic vesicles in some endings. The vesicles in affected small terminals were invariably flattened in shape (Fig. 5, insert). Larger terminals that demonstrated two or more active zones sometimes showed early degenerative changes as well. These took the form of a palisade type of arrangement of synaptic vesicles or an apparent enlargement of some round vesicles and a grouping of the vesicles towards the centre of the bouton. The vesicles in these larger terminals were often round in shape.

DISCUSSION

Cerebellar lesions

An ultrastructural analysis of degenerating terminal structures within the red nucleus of the rat revealed that degenerating profiles located within the magnocellular portion are predominantly in contact with cell bodies and proximal dendrites of giant and large rubral neurons. It has been established that the cerebellar projection to the magnocellular red nucleus in the rat originates entirely within the

---

Fig. 3(*a*). Electron micrograph of degenerating cerebellorubral terminals (arrows) occurring in a cluster. Each degenerating terminal is seen to be in contact with a separate dendritic profile. Terminals of this configuration are of similar size to those found on cell bodies and proximal dendrites. 3 days. × 9000. (*b*) Electron micrograph of a degenerating cerebellorubral terminal within the parvocellular portion of the red nucleus following a lesion of the deep cerebellar nuclei. This dentatorubral terminal is in contact with a small dendrite, and possesses an asymmetrical synaptic density, altered cell organelles and an electron-dense axoplasm. Degenerating terminals of this type are of comparable size to interpositorubral terminals of the magnocellular region, but the post-synaptic dendritic profile is smaller. 3 days. × 12000. (*c*) Electron micrograph of a degenerating dentatorubral terminal in contact with a medium sized dendrite. This electron-dense profile contains enlarged mitochondria and possesses an asymmetrical density. 3 days. × 9550.

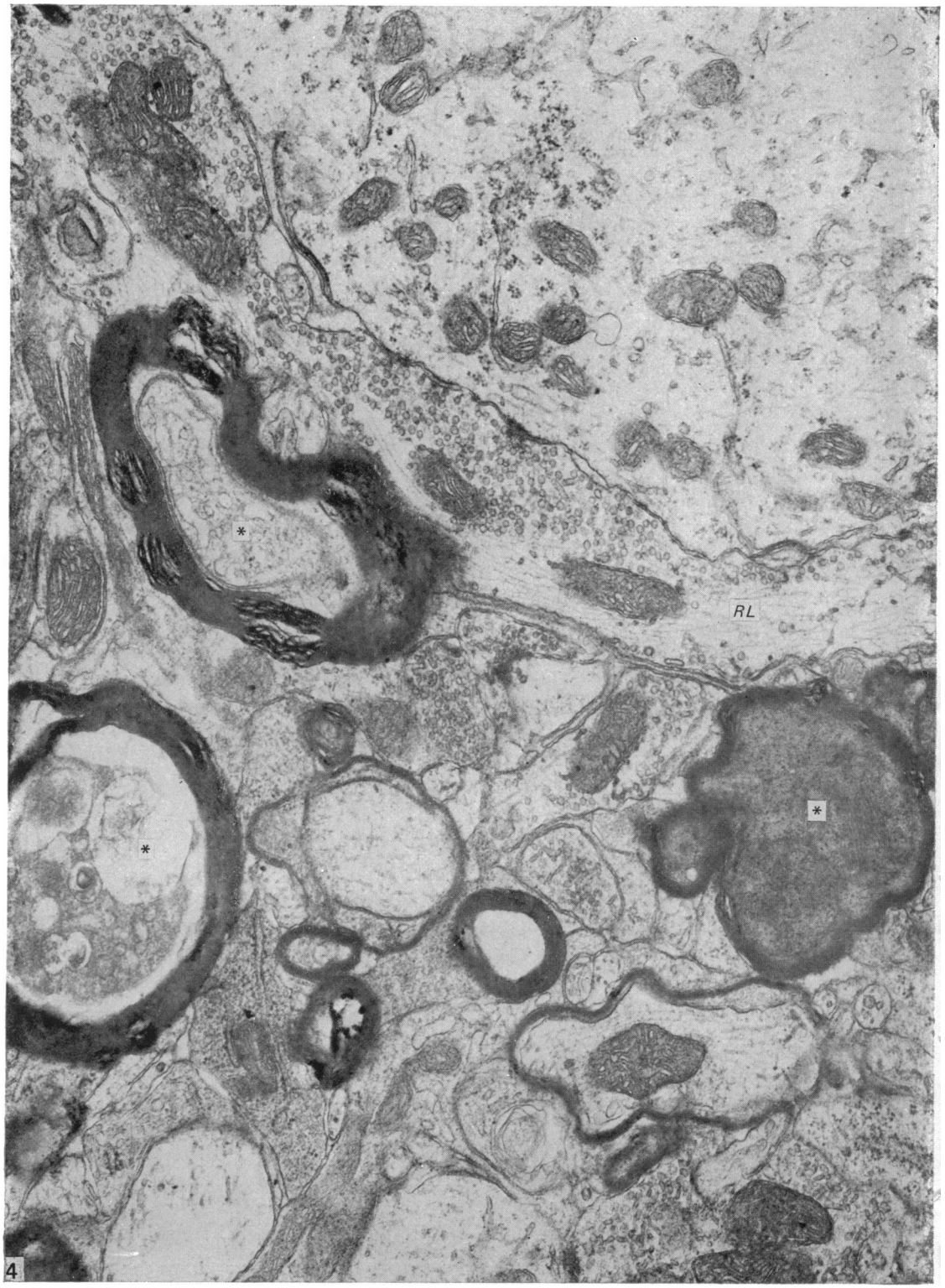

Fig. 4. Electron micrograph of the magnocellular subdivision contralateral to a total cerebellar lesion showing degenerating myelinated axons (*) and a normal large (*RL*) terminal containing rounded vesicles, mitochondria and neurofilaments, and making synaptic contact with the soma of a large neuron. 10 days. × 27750.

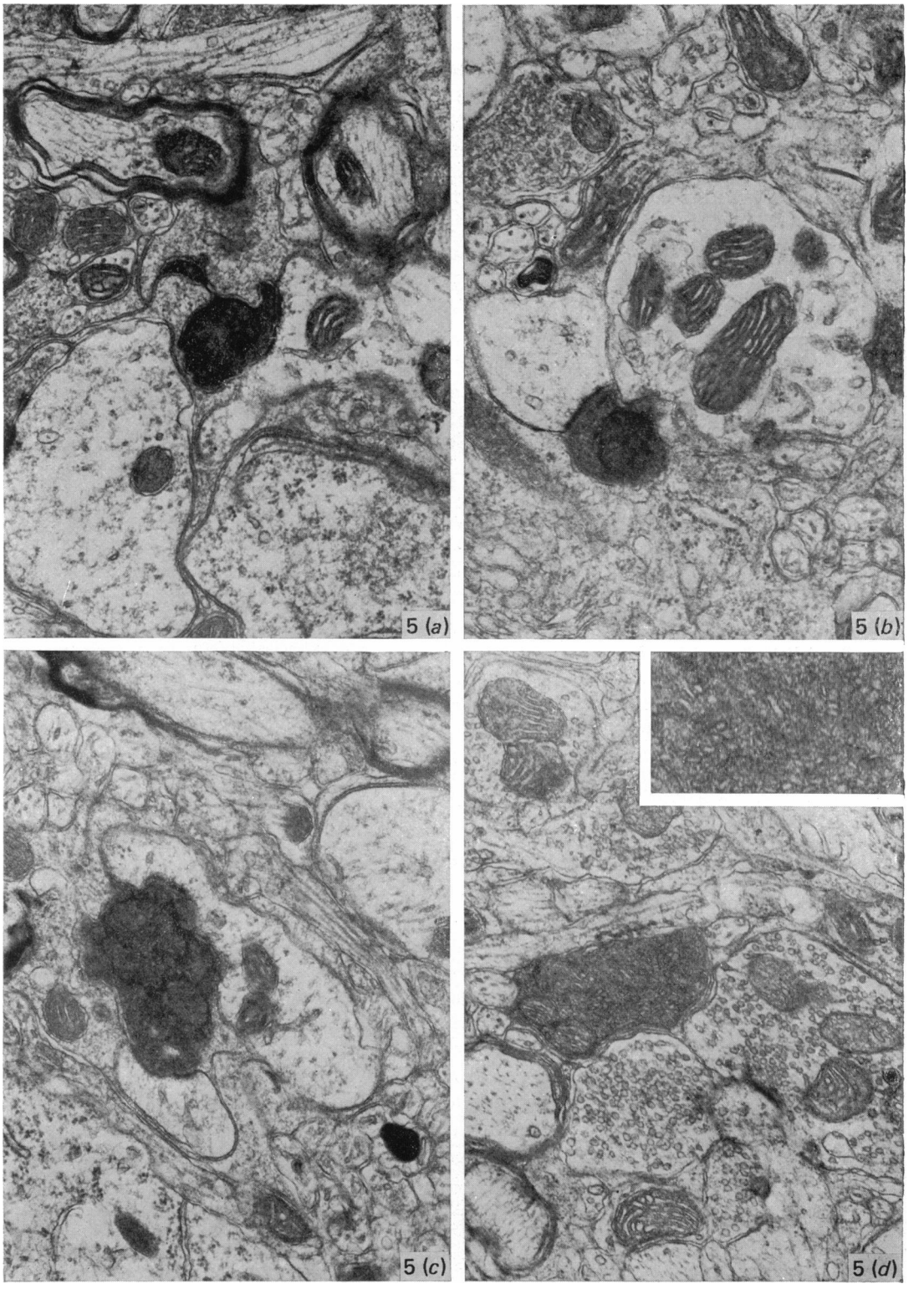

Fig. 5 (*a–d*). Synaptic terminals undergoing dark degeneration within the parvocellular part of the red nucleus 3 days following lesion of the sensorimotor cortex. The cortical terminals are in contact with distal dendrites or dendritic spines. In the early stages of degeneration (*d*) the synaptic vesicles are seen to be pleomorphic in shape (inset). (*a*) × 28 300; (*b*) × 24 750; (*c*) × 26 400; (*d*) × 26 400; inset × 60 000.

nucleus interpositus (Caughell & Flumerfelt, 1977). Furthermore, the large neurons in the magnocellular region give rise to all or most of the fibres in the rubrospinal tract (Gwyn & Flumerfelt, 1974). The results of this study therefore indicate the existence of an interpositorubrospinal pathway in this species. These results agree favourably with the data available for other species. It has been reported by Nakamura & Mizuno (1971) that interpositorubral fibres in the cat and rabbit terminate chiefly on the somata and proximal dendrites of magnocellular rubral neurons. This is also in accord with the electrophysiological evidence provided by Toyama, Tsukahara, Kosaka & Matsunami (1970) and Tsukahara, Murakami & Hultborn (1975).

In the North American opossum, it has also been demonstrated that the interpositorubral fibres mainly contact the somata and proximal dendrites of giant and large–medium size neurons (King, Dom, Conner & Martin, 1973). Unlike the degenerating interpositorubral terminals in the rat, the majority of the degenerating profiles observed in the opossum were large and ovoid (2–4 μm × 5–10 μm) or elongate (1 μm × 10–12 μm). Although terminals which are similar in form and location also occur in the rat (i.e. RL terminals), they were not seen undergoing degeneration in this study. It is possible that some of the degenerating terminals observed in the rat were RL terminals that had undergone extensive shrinkage during degeneration. This seems unlikely, however, since earlier forms of degeneration were not seen in RL terminals at shorter survival times. This possibility was investigated further by studying the long term effects of cerebellar lesions on the RL terminals. It was surmised that all terminals of cerebellar origin should eventually disappear with longer survival times, and conversely, persisting terminals could be considered to have originated elsewhere in the CNS. It was found that RL terminals were still in evidence up to 3 months following total transection of the brachium conjunctivum. Although this does not eliminate the possibility that some RL terminals are cerebellar in origin, it is likely that many of them arise instead from other afferent systems in the rat.

Although degenerating boutons within the magnocellular region of the rat were located predominantly on cell bodies and proximal dendrites, degenerating terminals occasionally were found in association with intermediate dendrites as well. Unlike the opossum and the cat (King *et al.* 1973; Nakamura, Mizuno & Konishi, 1978) boutons of this type occurred in clusters of 4–6 in number, each of which was in synaptic contact with a separate dendritic profile. Furthermore, degenerating terminals in the opossum and the cat were observed to undergo both hyperfilamentous and electron-dense types of degeneration while only the latter was characteristic of cerebellorubral terminals in the rat.

Light microscopic methods have revealed that the cerebellar projection to the parvocellular red nucleus originates in the dentate nucleus in the rat (Caughell & Flumerfelt, 1977). This pattern is consistent with electrophysiological data for the cat as well (Condé & Angaut, 1970; Oka & Jinnai, 1978). The present study has shown further that the dentatorubral endings terminate on intermediate and distal dendrites of the parvocellular neurons. The position of dentatorubral terminals in the rat contrasts with that observed in the opossum (King *et al.* 1973). In that species, lesions restricted to the nucleus lateralis (dentate nucleus) result in electron-dense degenerating terminals which are predominantly in contact with somata and proximal dendrites of large–medium neurons.

The apparent difference in the mode of termination of cerebellar afferents in the parvocellular and magnocellular parts of the rat red nucleus serves to emphasize the

essential differences in the organization and function of these two areas. Not only are they readily distinguishable by their cytoarchitecture, but also according to their afferent and efferent connections (Gwyn & Flumerfelt, 1974; Caughell & Flumerfelt, 1977). The magnocellular portion consists of predominantly large, multipolar neurons which receive numerous interpositus terminals on their somata and proximal dendrites, and which give rise in turn to axons which decussate and collectively form the rubrospinal tract. This tract has an excitatory action on contralateral flexor muscles and an opposite and inhibitory effect on extensor muscles (Massion, 1967). The magnocellular red nucleus therefore plays a role in adjusting the level of activity of different flexor muscles and in facilitating muscle tone. The parvocellular portion consists of predominantly small neurons which receive a moderate number of dentate terminals on their intermediate and distal dendrites and which give rise to axons that terminate ipsilaterally at medullary levels, particularly within the inferior olivary nucleus. The parvocellular portion, through its olivary connections, thereby plays a role in feedback control of the neocerebellar system.

The difference between the magnocellular and parvocellular portions is also apparent in the distribution of cortical terminals in the red nucleus. In the cat, the parvocellular part of the red nucleus is excited by the parietal association area of the cortex while the magnocellular part receives cortical afferents from the frontal motor area (Oka & Jinnai, 1978). In the rat the parvocellular region receives a projection from the sensorimotor cortex but the magnocellular part is devoid of cortical input (Gwyn & Flumerfelt, 1974; Brown, 1974). The cortical terminals observed in the present study were primarily small, contained pleomorphic vesicles, and terminated on distal dendrites. This pattern agrees favourably with the earlier light microscopic results which revealed a sparse pattern of diffuse degeneration throughout the parvocellular neuropil following cortical lesions. Moreover, in all species studied thus far there is general agreement that cortical terminals are localized on distal dendrites (King, Martin & Conner, 1972; Brown, 1974; Pizzini, Tredici & Miani, 1975; Tsukahara *et al.* 1975; Humphrey & Rietz, 1976). Due to their distal location, the corticorubral terminals are believed to play a role in regulating the background excitability of the rubral neurons by exerting a tonic modulatory facilitation upon their impulse discharges. The cerebellum, on the other hand, is responsible for exerting discrete excitatory influences via the dentate and interposed nuclei which are believed to function in the preprogramming of movement and the updating of ongoing movement respectively.

SUMMARY

The pattern and mode of termination of afferents to the red nucleus of the rat were investigated with the electron microscope. Lesions were placed by electrocautery in the sensorimotor cortex or were placed electrolytically in the deep cerebellar nuclei and brachium conjunctivum using a stereotaxic approach. With both types of lesion, degenerating fibres of passage, preterminal axons, and synaptic terminals were observed in greatest numbers on the third post-operative day. Following cerebellar lesions, degenerating terminals occurred on the cell bodies and proximal dendrites of large, multipolar neurons in the magnocellular portion of the red nucleus, and on intermediate and small dendrites in the parvocellular portion. It is concluded that the former are interpositus terminals while the latter are dentate (lateralis) terminals ending on rubrospinal and rubrobulbar neurons respectively. Following lesions of the sensorimotor cortex, small degenerating terminals were observed on the distal den-

drites and dendritic spines of parvocellular, rubrobulbar neurons. Large terminals containing round vesicles did not undergo degeneration following either type of lesion. These findings suggest the existence of an interpositorubro-spinal pathway in which the interpositus terminals exert a strong influence on the large, caudally placed rubrospinal neurons. The background excitability of the rostrally located rubrobulbar neurons is probably regulated by the distal cortical input while the more proximally located dentate terminals probably exert a stronger discrete influence over their activity.

The excellent technical assistance of Mrs J. Sholdice throughout this investigation is gratefully acknowledged. This study was supported by the Medical Research Council of Canada.

REFERENCES

BARNARD, J. W. & WOOLSEY, C. N. (1956). A study of localization in the corticospinal tracts of the monkey and rat. *Journal of Comparative Neurology* **105**, 25–50.

BROWN, L. T. (1974). Corticorubral projections in the rat. *Journal of Comparative Neurology* **154**, 149–168.

CAUGHELL, K. A. & FLUMERFELT, B. A. (1977). The organization of the cerebellorubral projection: an experimental study in the rat. *Journal of Comparative Neurology* **176**, 295–306.

CONDÉ, H. & ANGAUT, P. (1970). An electrophysiological study of the cerebellar projections to the nucleus ventralis lateralis thalami in the cat. II. Nucleus lateralis. *Brain Research* **20**, 107–119.

FLUMERFELT, B. A. & CAUGHELL, K. A. (1978). A horseradish peroxidase study of the cerebellorubral pathway in the rat. *Experimental Neurology* **58**, 95–101.

GWYN, D. G. & FLUMERFELT, B. A. (1974). A comparison of the distribution of cortical and cerebellar afferents in the red nucleus of the rat. *Brain Research* **69**, 130–135.

HUMPHREY, D. R. & RIETZ, R. R. (1976). Cells of origin of cortico-rubral projections from the arm area of primate motor cortex and their synaptic actions in the red nucleus. *Brain Research* **110**, 162–169.

KING, J. S., DOM, R. M., CONNER, J. & MARTIN, G. F. (1973). An experimental light and electron microscopic study of cerebellorubral projections in the opossum, *Didelphis marsupialis virginiana*. *Brain Research* **52**, 61–78.

KING, J. S., MARTIN, G. F. & CONNER, J. B. (1972). A light and electron microscopic study of corticorubral projections in the opossum, *Didelphis marsupialis virginiana*. *Brain Research* **38**, 251–265.

KREIG, W. J. S. (1946). Connections of the cerebral cortex. *Journal of Comparative Neurology* **84**, 221–275.

KUYPERS, H. G. J. M. & LAWRENCE, D. G. (1967). Cortical projections to the red nucleus and the brain stem in the rhesus monkey. *Brain Research* **4**, 151–188.

LEWIS, P. R. & SHUTE, C. C. D. (1966). The distribution of cholinesterase in cholinergic neurons demonstrated with the electron microscope. *Journal of Cell Science* **1**, 381–390.

LUFT, J. H. (1961). Improvements in epoxy resin embedding methods. *Journal of Biophysical and Biochemical Cytology* **9**, 409.

MABUCHI, M. & KUSAMA, T. (1966). The cortico-rubral projection in the cat. *Brain Research* **2**, 254–273.

MASSION, J. (1967). The mammalian red nucleus. *Physiological Reviews* **47**, 383–436.

NAKAMURA, Y. & MIZUNO, N. (1971). An electron microscopic study of the interposito-rubral connections in the cat and rabbit. *Brain Research* **35**, 283–286.

NAKAMURA, Y., MIZUNO, N. & KONISHI, A. (1978). A quantitative electron microscope study of cerebellar axon terminals on the magnocellular red nucleus neurons in the cat. *Brain Research* **147**, 17–27.

OKA, H. & JINNAI, K. (1978). Electrophysiological study of parvocellular red nucleus neurons. *Brain Research* **149**, 239–246.

PIZZINI, G., TREDICI, G. & MIANI, A. (1975). Corticorubral projection in the cat. An experimental electron-microscopic study. *Journal of Submicroscopic Cytology* **7**, 231–238.

REID, J. M., FLUMERFELT, B. A. & GWYN, D. G. (1975). An ultrastructural study of the red nucleus in the rat. *Journal of Comparative Neurology* **162**, 363–386.

REYNOLDS, E. S. (1963). The use of lead citrate at a high pH as an electron opaque stain in electron microscopy. *Journal of Cell Biology* **17**, 208–212.

RICHARDSON, K. C., JARETT, L. & FINKE, E. H. (1960). Embedding in epoxy resins for ultrathin sectioning in electron microscopy. *Stain Technology* **35**, 313–323.

RINVIK, E. & WALBERG, F. (1963). Demonstration of a somatotopically arranged cortico-rubral projection in the cat. *Journal of Comparative Neurology* **121**, 393–407.

SPURR, A. R. (1969). A low-viscosity epoxy resin embedding medium for electron microscopy. *Journal of Ultrastructure Research* **26**, 31.

TOYAMA, K., TSUKAHARA, N., KOSAKA, K. & MATSUNAMI, K. (1970). Synaptic excitation of red nucleus neurons by fibres from interpositus nucleus. *Experimental Brain Research* **11**, 187–198.

TSUKAHARA, N., MURAKAMI, F. & HULTBORN, H. (1975). Electrical constants of neurons of the red nucleus. *Experimental Brain Research* **23**, 49–64.

VAUGHN, J. E. & PETERS, A. (1966). Aldehyde fixation of nerve fibres. *Journal of Anatomy* **100**, 687.

WELKER, C. (1971). Microelectrode delineation of fine grain somatotopic organization of Sml cerebral neocortex in albino rat. *Brain Research* **26**, 259–275.

WOOLSEY, C. N. (1952). Patterns of localization in sensory and motor areas of the cerebral cortex. In *The Biology of Mental Health and Disease*, Milbank Memorial Fund, pp. 193–206. New York: Hoeber.

WOOLSEY, C. N. (1958). Organization of somatic sensory and motor areas of the cerebral cortex. In *Biological and Biochemical Bases of Behaviour* (ed. H. F. Harlow & C. N. Woolsey), pp. 63–81. Madison: University of Wisconsin Press.